Biointerface Research in Applied Chemistry
Open-Access Journal (ISSN: 2069-5837)

Article
Volume 13, Issue 2, 2023, 134
https://doi.org/10.33263/BRIAC132.134

Electrochemical Sensing of Uric Acid and Guanine Using a Graphite Paste Electrode of $NiMn_2O_4$ Spinel Nanoparticles

Susmita Pramanik [1], Parimal Karmakar [2], Dipak Kumar Das [1,*]

[1] Department of Chemistry, GLA University, 17 km stone NH-19 Delhi Mathura Highway Chaumuhan, Mathura, 281406 India
[2] Department of Life Sciences and Biotechnology, Jadavpur University, Kolkata, India
* Correspondence: deepak.das@gla.ac.in;

Scopus Author ID 57207705690
Received: 25.12.2021; Accepted: 24.01.2022; Published: 25.03.2022

Abstract: Guanine (GU) and uric acid (UA) each have their biological significance as an indicator and cause various serious disorders in the human body. Therefore, sensing their level in the human fluid is of paramount importance in monitoring serious human physiology disorders. In this regard, we developed an efficient electrochemical sensor from nanoparticles of nickel magnate (NPs-$NiMn_2O_4$) incorporated with graphite paste ($NiMn_2O_4$-NPs /GP) to detect both the GU and UA individually and simultaneously. Cyclic voltammetric (CV) and differential pulse voltammetric (DPV) techniques were employed to examine the electrochemical sensing ability of the $NiMn_2O_4$-NPs/GP sensor. The findings revealed that the detection limits of UA and GU were 400 and 400 Nm with linear ranges from 3.0 to 120 µM and 0.5 to 100 µM, respectively. Further, the influence of scan rate and pH of electrolyte on the sensing ability of prepared sensor was also systematically investigated.

Keywords: cyclic voltammetry; differential pulse voltammetry; electrochemical sensor; guanine; $NiMn_2O_4$ nanoparticles; uric acid.

1. Introduction

Guanine (GU) is one of the purines of the four nucleic acid building blocks and plays integral roles in cardiac rhythm, blood circulation, and neurotransmitter release. The blood level of GU can indicate the existence of cancer, deficiencies or mutations in the immune system, AIDS, epilepsy, myocardial cellular energy status, abnormal tissue degradation, and enzymatic and metabolic malfunctions [1,2]. Uric Acid (UA) is one of the main by-products of the metabolism of purine and is excreted by urine at 250mg dL-1 to 720 mg dL-1 concentration range [2]. Changes in GU in blood levels lead to hyperuricemia, gout, cardiovascular abnormalities, multiple sclerosis, oxidative stress, kidney diseases, high blood pressure, and Lesch-Nyan disease [3]. Simultaneous detections of both GU and UA are necessary as they co-exist in the body fluids and mutated DNA as they are both important markers for clinical medicine. Purine derivatives are a marker for agro -foods and human samples [4-7].

In this context, fluorescence spectrometry, mass spectroscopy, high-performance liquid chromatography (HPLC), ion-pairing liquid chromatography, flow in injection chemiluminescence-based sensors, micellar electro-kinetic chromatography, enzymatic analysis, and capillary zone electrophoresis are most commonly used for clinical detection for

both the GU and UA. However, all these methods are very time and labor-intensive, making them expensive. Hence, more affordable and versatile detection strategies are needed that can be used outside expensive laboratories, reducing sample collection, transportation, human errors owing to disparities, time constraints, etc. Sensors being small in size, portable, and easy to manufacture led to the surge in developmental research [8-13].

Within this agenda, modern electro-analytical sensors stand out among the numerous types of sensors being researched and developed due to their exceeding adaptability and sensitivity. The main principle here is biochemical reactions for the recognition of bio-molecules. Biomolecules and metabolic by-products have a distinctive electronic signature that can be detected by these sensors even in trace quantities and converted to analytical signals that can monitor physiological analytes in highly complex biological fluids or chemical analytes in commercial products. The full potential of sensor technology and development is evident in the race to fight the current COVID pandemic [2, 14-18].

The development of electrochemical sensors for UA and GU was hurdled due to the presence of interfering electroactive species in real samples, which influenced oxidation [19-20]. Challenges such as slow electron transfer, high overpotential, electrode surface fouling by oxidation product deposition, low reproducibility are frequently faced with the development of new electrodes [21,22]. However, they have numerous advantages, including being manufactured into inexpensive equipment with fast processing rates, collecting data quickly, and operating even if the sample of interest is complex, concentrated biological samples [23]. They can also be easily miniaturized and still produce high selectivity of detection at low concentrations [24]. This can be improved by modifying the electrode surfaces per need [7, 25]. For this purpose, graphite paste (GP) /carbon-paste electrodes (CPE) have become very popular for properties such as large potential domains, the ease with which they can be modified with the addition of other materials making into a paste having a satisfactory background current and fast surface regeneration [26-27]. Also, they are popular because of their chemical stability, slow biodegradation, low ohmic resistance, fast electrode surface renewability, mechanically robust. Thus, modification of GP with various materials like mixed oxides is capable of detecting samples in trace quantities using cheap and ready availability of oxide modifiers [9, 28-34].

We are particularly interested in developing oxide-based nanoparticles as sensor modifiers. The advantages of employing nano-sized oxides are good electrochemical conductivity due to defects in the lattice, a larger surface area having higher reaction centers, and also shows small over the potential of electrochemical reaction. The major parameters on which we focus are the ease and low cost of producing an electrode material that is chemically stable and has a long life. The prominent mixed oxides are spinel, orthoferrites, and perovskites [35-37]. All these nanoparticles of mixed oxides can be synthesized by combustion technique using simple laboratory chemicals [38-42]. So far, our team has developed a Lanthanum ortho-ferrite nano-material sensor for Dopamine detection [32] and a Copper Telluride based sensor for estimation of Epinephrine and Uric Acid [41,43]. Based on these sensors and their detection limits, we have developed a $NiMn_2O_4$ nanocomposite in a CPE as a novel sensor that can detect Uric acid and guanine efficiently at very low concentrations.

2. Materials and Methods

2.1. Chemicals and reagents.

Uric acid ($C_5H_4N_4O_3$), guanine ($C_5H_5N_5O$), and graphite powder were procured from Sigma Aldrich, USA. Nickel nitrate hexahydrate ($Ni(NO_3)_2,6H_2O$) manganese acetate anhydrous $(CH_3COO)_2Mn$), monoethanolamine (C_2H_7NO), nitric acid (HNO_3), and sucrose ($C_{12}H_{22}O_{11}$) are procured from Merck, India. The used chemicals were of analytical grade, and all solutions were prepared in de-ionized water or mentioned otherwise.

2.2. Synthesis of $NiMn_2O_4$ nanoparticles ($NiMn_2O_4$ -NPs).

The one-pot synthesis procedure was used to make nanoparticles (NPs) of $NiMn_2O_4$, 100 mL double distilled water was taken in a 1000 mL size beaker to which 1 gm nickel nitrate, 1.19 gm manganese acetate anhydrous, 5.6 gm mono-ethanolamine and 23 gm sucrose were added. 15 mL of concentrate nitric acid was added to it in order to ensure homogeneity. The solution was heated at 150-160^{o}C on a hot plate till the generation of black fluffy mass. This black fluffy mass obtained was ground in a mortar and pestle. Calcinations were conducted in a muffle furnace at 600^{o}C for 6-7 hours which then generated the $NiMn_2O_4$-NPs.

2.3. Fabrication of electrode for the sensor.

A paste with a uniform distribution of NiMn2O4-NPs and graphite (ratio 1:4, w/w) was prepared by mechanical mixing in a mortar-pastel after adding a few drops of paraffin oil. A capillary glass tube having an inner diameter of 2 mm and an outer diameter of 5 mm was utilized to fabricate the electrode. The tube was filled with this uniform paste of $NiMn_2O_4$-NPs and graphite and was tightly pressed using a thin metallic rod. For conductivity of current, a Pt wire was inserted at the opposite end of the capillary tube. The same methodology has been used for the fabrication of bare GP electrodes. The slurry of Al_2O_3 (0.6 mM) has been used to polish the composite surface. After washing with ethanol, the electrodes were subjected to desiccated drying under an N_2 atmosphere.

2.4. Apparatus and measurements.

For morphology and size analysis of the synthesized nps-$NiMn_2O_4$, high-resolution transmission electron microscope (HR-TEM; Tecnai G2 30 S-TWIN) and field emission scanning electron microscope (FESEM; Hitachi, SU-8010) were used. To perform electrochemical measurements with synthesized electrode ($NiMn_2O_4$/GP), Autolab101 (Netherlands) was used involving three-electrode system namely: Ag/AgCl electrode (also called as reference electrode), fabricated electrode (also called as a working electrode), and Pt electrode (known as a counter electrode) were used. Post optimization, as a supporting electrolyte, a phosphate buffer solution with pH 5.0 was used. Electrochemical studies were carried out at 25^{o}C. The used rates of the scan were 50 mVs^{-1} for DPV and 100 mVs^{-1} for CV. The voltage ranges used in the measurement were from 0.4 to 1.4 V for GU and from 0.0 to 0.8 V for UA. The simultaneous estimation of UA and GU at the surface of $NiMn_2O_4$-NPs/GP electrodes, the range of voltage was used 0.4 to 1.4 V for CV and 0.2 to 1.2 V for DPV methodologies.

3. Results and Discussion

3.1. Characterization of prepared nanoparticles (NPs) of $NiMn_2O_4$.

Figure 1 depicts a schematic presentation of a typical $NiMn_2O_4$-NPs based sensor electrode fabrication process. Combustion and heat treatment procedures were used to prepare $NiMn_2O_4$-NPs based sensor electrodes.

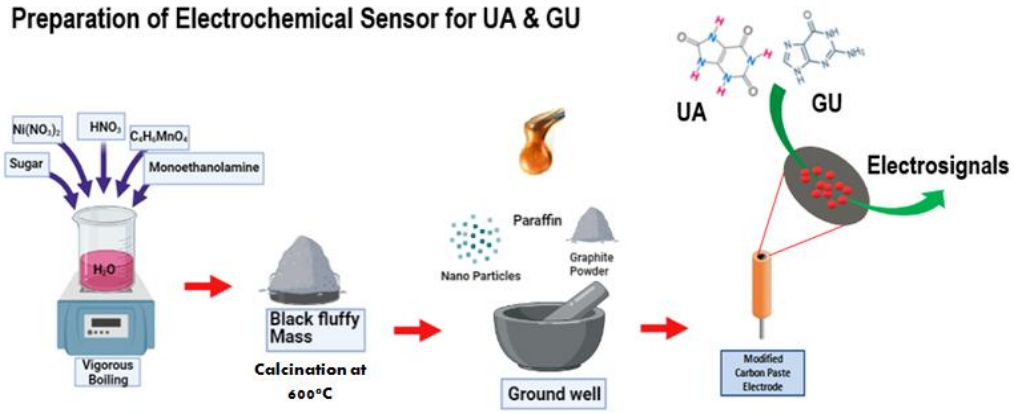

Figure 1. Systematic illustration of $NiMn_2O_4$-NPs based sensor electrode.

Further, various analytical techniques such as XRD, FE-SEM, elemental mapping, and TEM were used to analyze the produced np-$NiMn_2O_4$. The crystalline structure and chemical compositions of $NiMn_2O_4$-NPs are determined using XRD patterns (Fig. 2a). The appeared diffraction peaks at 2$\boldsymbol{\theta}$ values of 19.7°, 37.2°, 44.0°, 47.2°, 56.1°, 70.5°, 77.9°, and 84.1°, as compared to previously reported work [44].

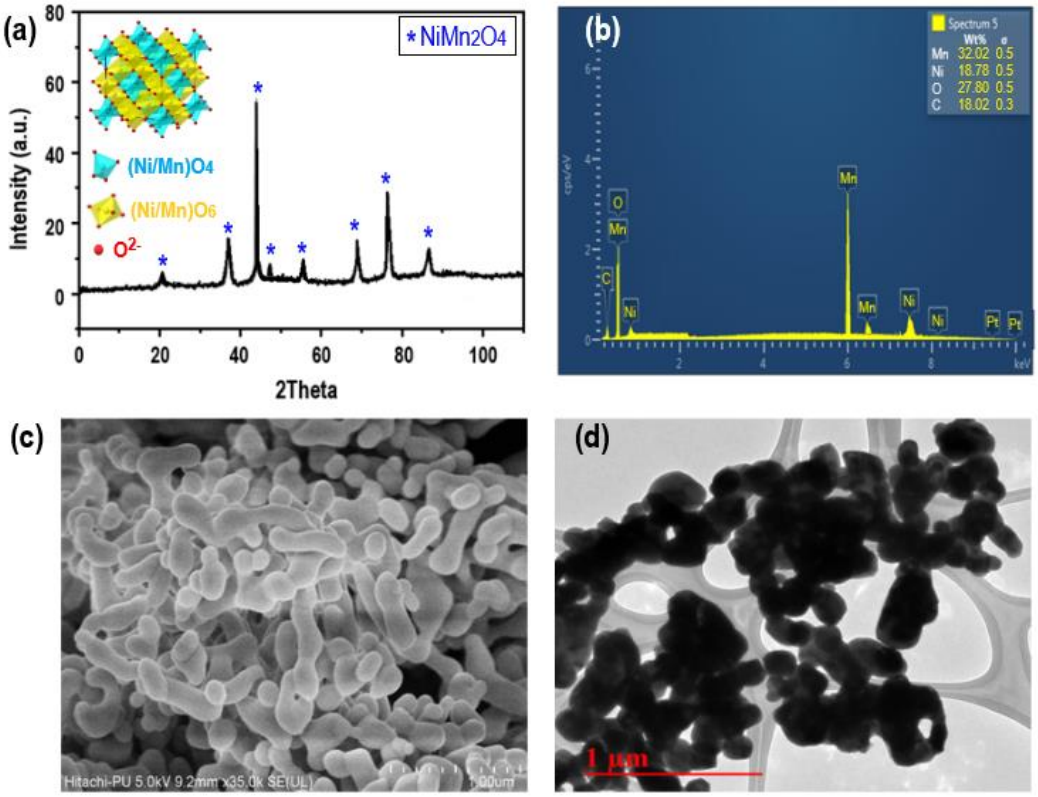

Figure 2. (**a**) XRD pattern of synthesized $NiMn_2O_4$ NPs (inset figure is indicating the crystal model of $NiMn_2O_4$), (**b**) Elemental mapping picture of $NiMn_2O_4$ NPs, (**c**) FESEM, (**d**) TEM images of synthesized $NiMn_2O_4$ NPs.

The crystal structure of the spinel $NiMn_2O_4$-NPs was shown in the inset image in Figure 2a, which adopted a cubic structure of Ni/Mn ions with Ni:Mn=1:2 embedded in the interstices of oxygen tetrahedron and octahedron stacking. The close-packed oxygen anions (O^{2-}) make up the cubic lattice in which these cations are embedded. EDX of the sample shown in Figure 2b presented the elemental picture of $NiMn_2O_4$-NPs, indicating the atomic ratio of Ni, Mn, and O-atoms as expected. Further, the morphology and structure of prepared np-$NiMn_2O_4$ were characterized by FE-SEM. The FE-SEM image (Figure 2c) clearly indicates that these NiMn2O4-NPs possessed the cubic crystal structured morphology with the size ranging between 50 to 60 nm, as supported by the TEM image (Figure 2d).

3.2. Sensing performance of the prepared electrochemical sensor.

3.2.1. Electro-investigations of $NiMn_2O_4$-NPs /GP Composite and bare GP Electrode.

At the preliminary label, the electrochemical property of the modified electrode ($NiMn_2O_4$-NPs /GP) was studied using a mixture of $[Fe(CN)_6]^{-4}$/ $[Fe(CN)_6]^{-3}$ as a standard redox system. Cyclic voltammograms of both electrodes displayed a current (oxidation) value of 108 µA and 87 µA in case $NiMn_2O_4$ –NPs /GP electrodes and GP electrodes, respectively. The cyclic voltammograms for both electrodes using 3 mM $K_4[Fe(CN)_6]$ have been presented in Figure 2. This revealed composite electrodes' efficient electrocatalytic chemical activity over simple GP electrodes.

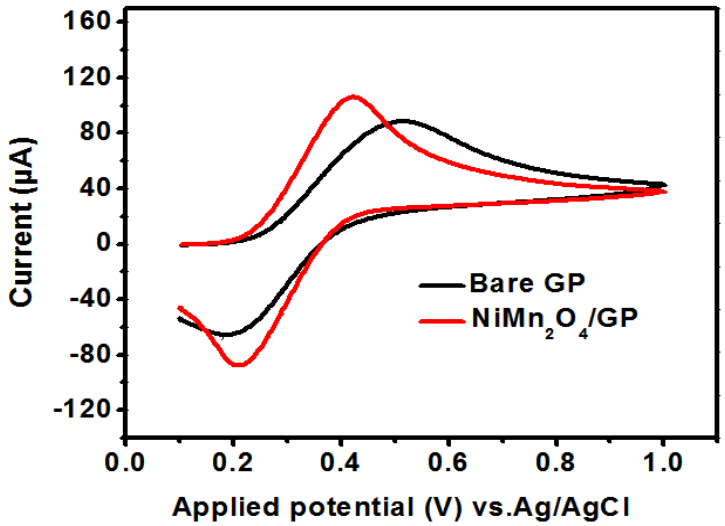

Figure 3. Cyclic Voltammogram plots as obtained under 3 mM V $[Fe(CN)_6]^{-4}$/$[Fe(CN)_6]^{-3}$ redox system.

3.2.2. Electrocatalytic Oxidation of GU and UA at $NiMn_2O_4$-NPs /GP Electrode Surface.

Voltammograms were recorded to study the responses of sensors of fabricated electrodes towards bio-molecules UA and GU individually and also in a mixture. The cyclic voltammogram of $NiMn_2O_4$-NPs/GP electrodes was obtained for UA (Figure 4a) and GU (Figure 4b). Peak values of oxidation potentials at $NiMn_2O_4$-NPs /GP electrode surface were found to be 583mV for UA and 978mV for GU. The peak current value for UA was 9.31 µA, and GU was 10.74 µA at $NiMn_2O_4$-NPs /GP electrode. For only GP electrode, the peak current was found to be 6.05 µA for UA and 5.45 µA for GU, respectively (Figure 4c). On the other hand, the sensing capacity of the electrode in a mixture of UA and GU, differential pulse voltammogram was recorded in the mixture of 100 µM UA and 100 µM GU was recorded. From Figure 4, it can be easily concluded that the newly developed electrode showed two

separated UA and GU peaks with a good separation difference, i.e., 434 mV between both bio-molecules (Figure 4d). These observations revealed that efficient electrocatalytic activities introduce better detection and faster electron transfer. After optimization, an optimum scan rate for all CV measurements was performed at 100 mVs-1. In the case of DPV measurement, the scan rate was performed at 50 mVs^{-1} under pre-defined conditions [5 mV as step potential; 40 mV as modulation amplitude, 0.02 s as modulation time, and 0.01 s as interval time].

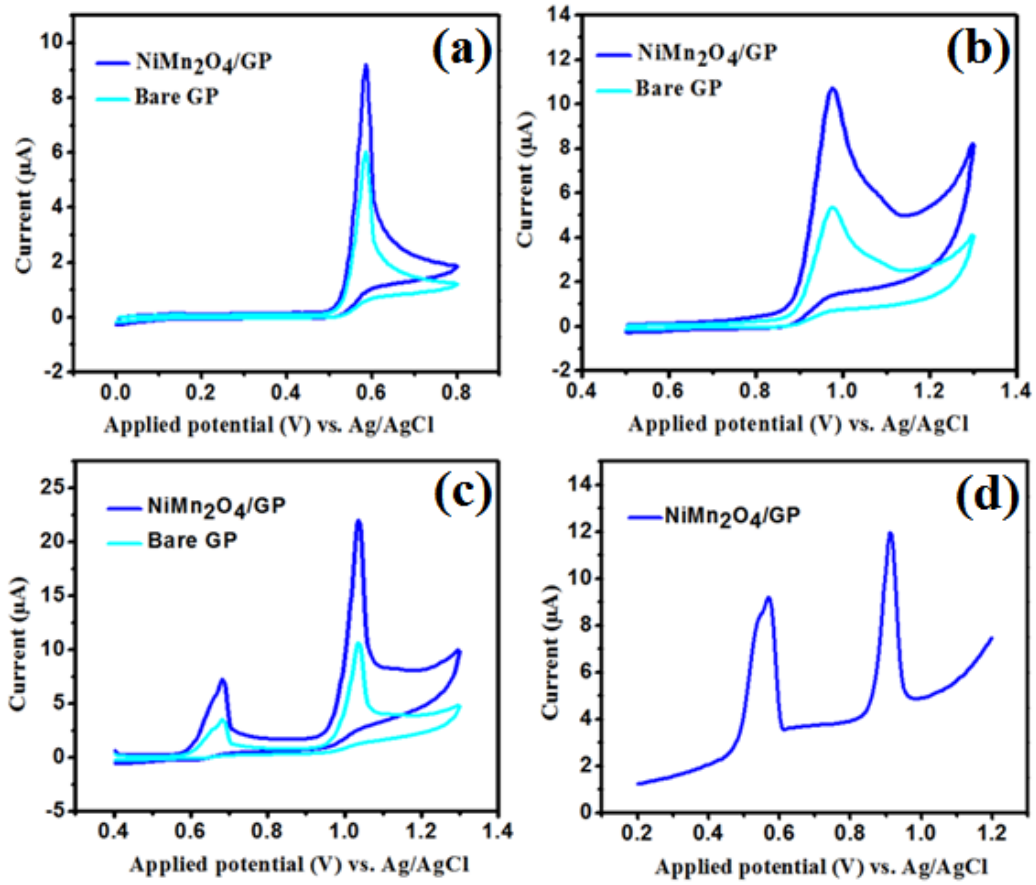

Figure 4. Cyclic voltammogram plots of (**a**) 0.1 mM of UA; (**b**) 0.1 mM of GU; (**c**) A combination of 0.1 mM UA and 0.1 mM GU; (**d**) DPV plot for a combination of 0.1 mM UA and 0.1 mM GU [*Background electrolyte: 0.1M phosphate (pH 5.0); scan rate of CV: 100 mVs^{-1}; scan-rate of DPV:50 mVs^{-1}].

Cyclic voltammograms were recorded from 0.0 to 0.8 V for UA. Similarly, cyclic voltammograms of GU were recorded from 0.4 to 1.4 V for the simultaneous estimation of GU and UA at $NiMn_2O_4$-NPs /GP electrodes. The voltage was changed between 0.4 to 1.4 V for CV and from 0.2 to 1.2 V for DPV, respectively.

3.2.3. Effect of pH and scan rate on the oxidation of UA and GU at $NiMn_2O_4$-NPs/GP electrodes.

In the electrochemical analysis of all these bio-molecules, supporting electrolytes plays an important role [45]. Cyclic voltammetry recorded the effect of pH on the peak potential and peak current of GU and UA molecules. The experiments were performed in phosphate buffer solution with pH variation from 4.0-6.0 at an interval of 0.5. The insets of Figures 5a and 5b display the variations of the peak current with pH.

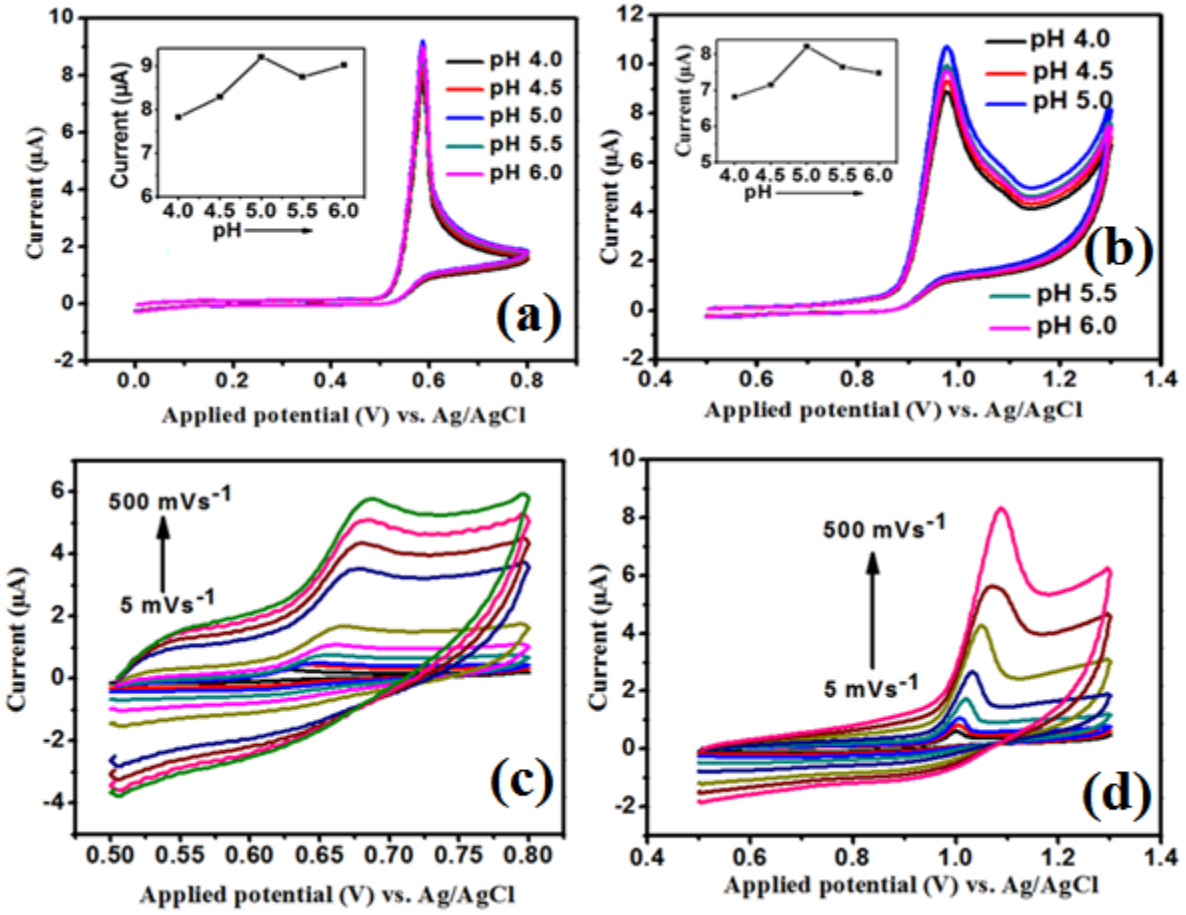

Figure 5. pH variation from pH 4 to 6 (**a**) for UA, current value shown in inset, (**b**) for GU, current value shown in inset, and the scan rate ranging between 5-500 mVs^{-1}, (**c**) for UA (0.1mM); (**d**) for GU (0.1mM) at $NiMn_2O_4$-NPs/GP electrode.

Values of GU and UA increase from pH=4 to pH=5. Above pH=5 current was decreasing with the increase of pH value of supporting electrolyte. This variation may be the outcome of generating various anions of analytes with increasing pH. The optimum pH was found to be 5. Thus, all experiments related to CV and DPV experiments were performed at pH=5.

Variation of scan rates from 05.0 mVs^{-1} to 500.0 mVs^{-1} was used in cyclic voltammetric measurement to study its effect on electrocatalytic oxidation on GU and UA. The scan rate was positively correlated with a linear increment in the peak current (Fig. 5c-d).

3.2.4. Simultaneous estimation of UA & GU at prepared composite $NiMn_2O_4$-NPs/GP electrode.

A controlled DPV measurement has been performed for obtaining a higher resolution optimum peak current essential for the simultaneous estimations of GU and UA, and results presented graphically (Figures 6a-b). In DPV method, fixed concentrations of GU were maintained at 100 µM with a varying UA concentration ranging between 3-120 µM. The study is presented in Fig. 6a. The linear range was found at a concentration range of 1-40 µM (R^2 = 0.965) and can be represented as equation 1:

$$(I_{UA})\ y = 0.028UA + 0.115 \qquad \text{eq. 1}$$

The second linear range (R^2 = 0.973) was found at the concentration range 40-120 µM as shown in equation 2:

(I_{UA}) y = 0.002UA + 0.144 eq. 2

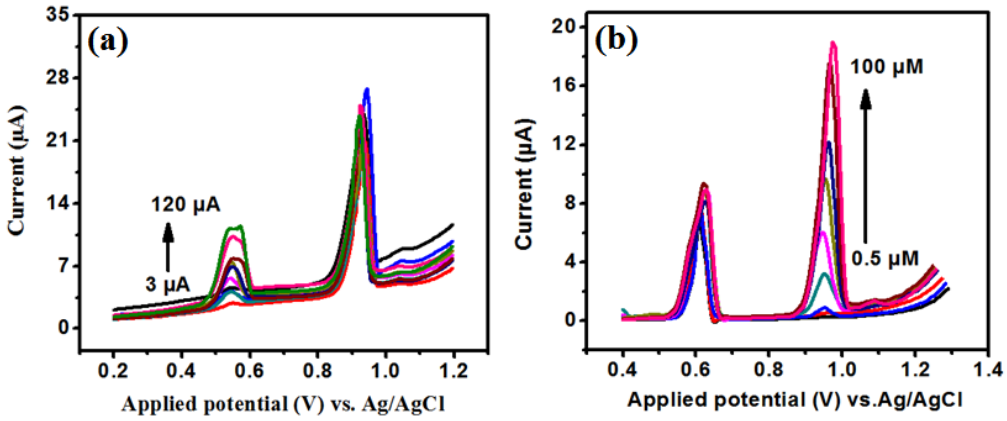

Figure 6. Oxidation current vs voltage plots at (**a**) varying concentrations ofUA (1 µM-120 µM) [Concentration of GU:100 µM]; (**b**) varying concentrations of GU from (0.5 µM-100 µM)[Concentration of UA: 100 µM].

An increase in oxidation peak current (I_{UA}) was found to be facilitated with an increase in the concentrations of GU and UA. The lowest detection limits for GU and UA were noted to be 300 nM and 400 nM, respectively.

3.2.5. Comparative study with the previously developed electrode.

The comparative study of the response of $NiMn_2O_4$-NPs/GP and previously developed electrodes has been done by several investigators. Hui *et al.* used PANI/Mn2O modified electrode [46], Yang *et al.* used $NiCoO_2$/GPE modified electrode [47], Liu *et al*. used PI-mox GO/GCE modified electrode [19], Kumar *et al*. used CTAB/GCE modified electrode [27], Yari *et al.* used TAN-Ag NP-PANF/CPE modified electrode [26], Jesney *et al.* used p-PTSA/GCE modified electrode [2]. Similarly, Cruz *et al.* used UO x-poly(4-ASA)-PB-CSPE modified electrode [6], and Beitollahi *et al.* also used GO/Fe_3O_4@SiO_2/CSPE modified electrode [7]. The detection limit and linearity range of the above-mentioned investigations have been presented in Table 1. Our values are comparable or better than all these presented reports.

Table 1. Comparison of linear range and detection limits with various electrodes along with np-NiMn2O4 /GP electrode.

Modified Electrodes	Guanine		Uric acid		References
	Linear Detection range (µM)	Detection Limit (nm)	Linear Detection range (µM)	Detection limit (nm)	
p-PTSA/GCE	10-100	350	10-100	5880	[2]
UO x-poly(4-ASA)-PB-CSPE	-	-	10-200	3000	[5]
GO/Fe_3O_4@SiO_2/CSPE	-	-	0.75-300	570	[6]
PImox GO/GCE	3.3-103.3	480	3.6-249.6	590	[16]
TAN-Ag NP-PANF/CPE	0.9-140	3000	-	-	[20]
PANI/MnO_2/GCE	10-100	4800	-	-	[36]
$NiCoO_2$/GCE	-	-		5300	[37]
CTAB/GCE	Feb-60	300	5-125	1700	[38]
np$NiMn_2O_4$/GP	0.5-100	300	03–120	400	Present work

3.2.6. Reproducibility of the prepared electrode.

To check reproducibility as seen in most recent research works of fabricated electrodes [48], five electrodes were made using identical conditions. The almost similar response-of all five electrodes were noted by CV analysis (Fig. 7). The stability of the electrode was studied by post storage at a temperature of 30°C ± 1°C for 40 days, and it retained 97% of the initial response. To check repeatability, 10 experiments were performed under the same experimental condition with the same electrode and found no change of initial response. Citric acid, ascorbic acid, oxalic acid, and some common metal ions exhibited nil interfering effect even with 100 µM of their concentrations. Based on these above findings, it could be concluded that $NiMn_2O_4$-NPs/GP modified electrode was highly appropriate for detecting GU and UA.

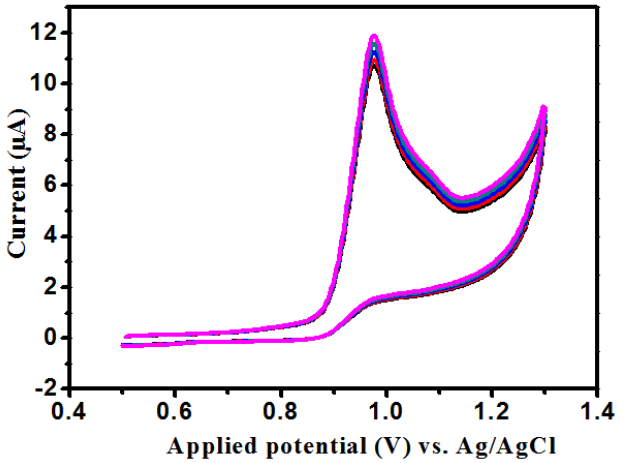

Figure 7. Reproducibility of the prepared electrode by preparing five electrodes using a similar fabrication method.

3.2.7. Real sample analysis using $NiMn_2O_4$-NPs /GP composite electrode.

The urine & human serum samples were selected to estimate UA in the real sample to test the efficiency of the composite electrode. After centrifuging at 4000 rpm, the samples were diluted with phosphate buffer (pH: 5.0) and tested using the prepared electrode. The recovery values for UA in urine and blood serum samples were noted to be 100.5 and 99.7%, respectively, using the following equation (Eq 3) [33]:

$$\text{Recovery}^2 = \frac{\text{Found}(\mu M) - \text{Diluted biologial fluids/pharmaceutical sample}(\mu M)}{\text{Spiking}(\mu M)} \times 100\% \qquad \text{eq. 3}$$

In the case of GU, the recovery values were found to be 101.1% in urine and99.6% in human serum samples. The results are summarized in Table 2.

Table 2. Determination of UA and GU in real samples at modified $NiMn_2O_4$ electrode (n=3).

Electrode	Sample	Sample Type (Original/Diluted) (µM)	Spiking(µM)	Found(µM)	R.S.D[1] (%)	Recovery[2] (%)
	Urine Sample					
	UA	20	30	50.5	1.92	100.5
	GU	0	50	50.1	1.54	100.1
$NiMn_2O_4$NPs /GP	**Human serum sample**					
	UA	20	30	49.8	1.4	99.7
	GU	0	50	50.3	1.7	99.6

Relative standard deviation[1].

4. Conclusions

In this study, NiMn2O4-NPs modified GP electrode fabrication has been reported, along with the synthesis procedure of nanoparticles of $NiMn_2O_4$ by simple combustion method using ethanolamine and sugar as fuel. The size in the nano range has been confirmed by advanced analytical techniques like FESEM & TEM by 50-60 nm. The electrochemical activities of modified graphite paste electrodes were analyzed using CV & DPV techniques to estimate biological molecules GU and UA. The $NiMn_2O_4$-NPs based composite electrodes showed promising results towards the determination of UA & GU with a detection limit (GU:300 nM; UA: 400 nM), lower than previously reported works. The developed composite electrode had good selectivity, excellent stability, and reproducibility. The synthesis of spinel powder is simple with superior sensitivity of detection. The proposed $NiMn_2O_4$-NPs /GP composite electrode may find for the estimation of UA and GU for diagnostic used in medical science.

Funding

This research received no external funding.

Acknowledgments

All the authors acknowledge Dr. Anuj Kumar, Dr. Yogendra Kumar, and the management of GLA University, Mathura (India), for providing academic and technical support and Jadavpur University, Kolkata (India) for experimental and technical support.

Conflict of Interest

The authors declare no conflict of interest.

References

1. Sharma, V.K.; Jelen, F.; Trnkova, L. Functionalized Solid Electrodes for Electrochemical Biosensing of Purine Nucleobases and Their Analogues: A Review. *Sensors* **2015**, *15*, 1564-1600, https://doi.org/10.3390/s150101564.
2. Jesny, S.; Menon, S.; Girish Kumar, K. Simultaneous determination of guanine and adenine in the presence of uric acid by a poly(para toluene sulfonic acid) mediated electrochemical sensor in alkaline medium. *RSC Advances* **2016**, *6*, 75741-75748, https://doi.org/10.1039/c6ra13567f.
3. Chakkarapani, L.D.; Arumugam, S.; Brandl, M. Layer-by-layer sensor architecture of polymers and nanoparticles for electrochemical detection of uric acid in human urine samples. *Materials Today Chemistry* **2021**, *22*, 100561, https://doi.org/https://doi.org/10.1016/j.mtchem.2021.100561.
4. Gao, S.; Li, H.; Li, M.; Li, C.; Qian, L.; Yang, B. A gold-nanoparticle/horizontal-graphene electrode for the simultaneous detection of ascorbic acid, dopamine, uric acid, guanine, and adenine. *Journal of Solid State Electrochemistry* **2018**, *22*, 3245-3254, https://doi.org/10.1007/s10008-018-4019-7.
5. Yan, Q.; Zhi, N.; Yang, L.; Xu, G.; Feng, Q.; Zhang, Q.; Sun, S. A highly sensitive uric acid electrochemical biosensor based on a nano-cube cuprous oxide/ferrocene/uricase modified glassy carbon electrode. *Scientific Reports* **2020**, *10*, 10607, https://doi.org/10.1038/s41598-020-67394-8.
6. da Cruz, F.S.; de Souza Paula, F.; Franco, D.L.; dos Santos, W.T.P.; Ferreira, L.F. Electrochemical detection of uric acid using graphite screen-printed electrodes modified with Prussian blue/poly(4-aminosalicylic acid)/Uricase. *Journal of Electroanalytical Chemistry* **2017**, *806*, 172-179, https://doi.org/10.1016/j.jelechem.2017.10.070.

7. Beitollahi, H.; Nejad, F.G.; Shakeri, S. GO/Fe_3O_4@SiO_2 core–shell nanocomposite-modified graphite screen-printed electrode for sensitive and selective electrochemical sensing of dopamine and uric acid. *Analytical Methods* **2017**, *9*, 5541-5549, https://doi.org/10.1039/c7ay01226h.
8. Shashikumara, J.K.; Kumara Swamy, B.E.; Chetankumar, K. Sensitive and selective sensor for 3, 4-dihydroxyphenethylamine and uric acid at poly (Orange CD) modified carbon paste electrode. *Chemical Data Collections* **2021**, *32*, 100661, https://doi.org/10.1016/j.cdc.2021.100661.
9. Kumar, Y.; Pradhan, S.; Pramanik, S.; Bandyopadhyay, R.; Das, D.K.; Pramanik, P. Efficient electrochemical detection of guanine, uric acid and their mixture by composite of nanoparticles of lanthanides ortho-ferrite $XFeO_3$ (X = La, Gd, Pr, Dy, Sm, Ce and Tb). *Journal of Electroanalytical Chemistry* **2018**, *830-831*, 95-105, https://doi.org/10.1016/j.jelechem.2018.10.021.
10. Chang, J.; Xiao, W.; Liu, P.; Liao, X.; Wen, Y.; Bai, L.; Li, L.; Li, M. Carboxymethyl cellulose assisted preparation of water-processable halloysite nanotubular composites with carboxyl-functionalized multi-carbon nanotubes for simultaneous voltammetric detection of uric acid, guanine and adenine in biological samples. *Journal of Electroanalytical Chemistry* **2016**, *780*, 103-113, https://doi.org/https://doi.org/10.1016/j.jelechem.2016.09.013.
11. Mendes, C.H.S.; Montenegro, J.G.S.; Queiroz, N.L.; Moreira, T.C.S.; Nascimento, V.B.; Oliveira, S.C.B. Electrochemical Detection of Guanine-methylation Using Glassy Carbon Electrode. *Electroanalysis* **2020**, *32*, 19-28, https://doi.org/https://doi.org/10.1002/elan.201900223.
12. Income, K.; Ratnarathorn, N.; Khamchaiyo, N.; Srisuvo, C.; Ruckthong, L.; Dungchai, W. Disposable Nonenzymatic Uric Acid and Creatinine Sensors Using μPAD Coupled with Screen-Printed Reduced Graphene Oxide-Gold Nanocomposites. *International Journal of Analytical Chemistry* **2019**, *2019*, 3457247, https://doi.org/10.1155/2019/3457247.
13. Turkkan, G.; Bas, S.Z.; Atacan, K.; Ozmen, M. An electrochemical sensor based on a Co3O4–ERGO nanocomposite modified screen-printed electrode for detection of uric acid in artificial saliva. *Analytical Methods* **2022**, *14*, 67-75, https://doi.org/10.1039/d1ay01744f.
14. Senf, B.; Yeo, W.-H.; Kim, J.-H. Recent Advances in Portable Biosensors for Biomarker Detection in Body Fluids. *Biosensors* **2020**, *10*, 127, https://doi.org/10.3390/bios10090127.
15. Bhalla, N.; Pan, Y.; Yang, Z.; Payam, A.F. Opportunities and Challenges for Biosensors and Nanoscale Analytical Tools for Pandemics: COVID-19. *ACS Nano* **2020**, *14*, 7783-7807, https://doi.org/10.1021/acsnano.0c04421.
16. Li, Y.; Liu, J. Sensing guanine and its derivatives: From molecular recognition to applications. *Sensors and Actuators Reports* **2020**, *2*, 100020, https://doi.org/10.1016/j.snr.2020.100020.
17. Zhang, J.; Han, D.; Wang, S.; Zhang, X.; Yang, R.; Ji, Y.; Yu, X. Electrochemical detection of adenine and guanine using a three-dimensional WS_2 nanosheet/graphite microfiber hybrid electrode. *Electrochemistry Communications* **2019**, *99*, 75-80, https://doi.org/10.1016/j.elecom.2019.01.007.
18. Mao, B.; Qian, L.; Govindhan, M.; Liu, Z.; Chen, A. Simultaneous electrochemical detection of guanine and adenine using reduced graphene oxide decorated with AuPt nanoclusters. *Microchimica Acta* **2021**, *188*, 276, https://doi.org/10.1007/s00604-021-04926-7.
19. Liu, X.; Zhang, L.; Wei, S.; Chen, S.; Ou, X.; Lu, Q. Overoxidized polyimidazole/graphene oxide copolymer modified electrode for the simultaneous determination of ascorbic acid, dopamine, uric acid, guanine and adenine. *Biosensors and Bioelectronics* **2014**, *57*, 232-238, https://doi.org/10.1016/j.bios.2014.02.017.
20. Papavasileiou, A.V.; Trachioti, M.G.; Hrbac, J.; Prodromidis, M.I. Simultaneous determination of guanine and adenine in human saliva with graphite sparked screen-printed electrodes. *Talanta* **2022**, *239*, 123119, https://doi.org/10.1016/j.talanta.2021.123119.
21. Slate, A.J.; Brownson, D.A.C.; Abo Dena, A.S.; Smith, G.C.; Whitehead, K.A.; Banks, C.E. Exploring the electrochemical performance of graphite and graphene paste electrodes composed of varying lateral flake sizes. *Physical Chemistry Chemical Physics* **2018**, *20*, 20010-20022, https://doi.org/10.1039/c8cp02196a.
22. Tigari, G.; Manjunatha, J.G. A surfactant enhanced novel pencil graphite and carbon nanotube composite paste material as an effective electrochemical sensor for determination of riboflavin. *Journal of Science: Advanced Materials and Devices* **2020**, *5*, 56-64, https://doi.org/10.1016/j.jsamd.2019.11.001.
23. Liu, H.; Jamal, R.; Abdiryim, T.; Simayi, R.; Liu, L.; Liu, Y. Carboxylated Cellulose as a Soft Template Combined with PEDOT Derivatives in [BMIM]Cl: A Competent Biosensor for Detection of Guanine and Uric Acid in the Blood. *ACS Sustainable Chemistry & Engineering* **2021**, *9*, 5860-5871, https://doi.org/10.1021/acssuschemeng.0c09259.

24. Guo, H.; Zhang, T.; Wang, M.; Sun, L.; Zhang, J.; Yang, M.; Yang, F.; Wu, N.; Yang, W. Electrochemical behavior of MOF-801/MWCNT-COOH/AuNPs: A highly selective electrochemical sensor for determination of guanine and adenine. *Colloids and Surfaces A: Physicochemical and Engineering Aspects* **2021**, *627*, 127195, https://doi.org/10.1016/j.colsurfa.2021.127195.
25. Charithra, M.M.; Manjunatha, J.G.G.; Raril, C. Surfactant Modified Graphite Paste Electrode as an Electrochemical Sensor for the Enhanced Voltammetric Detection of Estriol with Dopamine and Uric acid. *Adv Pharm Bull* **2020**, *10*, 247-253, https://doi.org/10.34172/apb.2020.029.
26. Yari, A.; Saidikhah, M. Trithiane silver-nanoparticles-decorated polyaniline nanofibers as sensing element for electrochemical determination of Adenine and Guanine in DNA. *Journal of Electroanalytical Chemistry* **2016**, *783*, 288-294, https://doi.org/10.1016/j.jelechem.2016.10.063.
27. Kumar, M.; Fu, Y.; Wang, M.; Swamy, B.E.K.; Jayaprakash, G.K.; Zhao, W. Influence of cationic surfactant cetyltrimethylammonium bromide for electrochemical detection of guanine, uric acid and dopamine. *Journal of Molecular Liquids* **2021**, *321*, 114893, https://doi.org/10.1016/j.molliq.2020.114893.
28. Bellido-Milla, D.; Cubillana-Aguilera, L.M.; El Kaoutit, M.; Hernández-Artiga, M.P.; Hidalgo-Hidalgo de Cisneros, J.L.; Naranjo-Rodríguez, I.; Palacios-Santander, J.M. Recent advances in graphite powder-based electrodes. *Analytical and Bioanalytical Chemistry* **2013**, *405*, 3525-3539, https://doi.org/10.1007/s00216-013-6816-2.
29. Benvidi, A.; Nafar, M.T.; Jahanbani, S.; Tezerjani, M.D.; Rezaeinasab, M.; Dalirnasab, S. Developing an electrochemical sensor based on a carbon paste electrode modified with nanocomposite of reduced graphene oxide and $CuFe_2O_4$ nanoparticles for determination of hydrogen peroxide. *Materials Science and Engineering: C* **2017**, *75*, 1435-1447, https://doi.org/10.1016/j.msec.2017.03.062.
30. Fekry, A.M.; Shehata, M.; Azab, S.M.; Walcarius, A. Voltammetric detection of caffeine in pharmacological and beverages samples based on simple nano- Co (II, III) oxide modified carbon paste electrode in aqueous and micellar media. *Sensors and Actuators B: Chemical* **2020**, *302*, 127172, https://doi.org/10.1016/j.snb.2019.127172.
31. Abdel-Raoof, A.M.; Elsonbaty, A.; Abdulwahab, S.; Hassan, W.S.; Eissa, M.S. Potentiometric determination of amprolium drug at a carbon nanotubes/nickel oxide nanoparticles paste electrode. *Microchemical Journal* **2021**, *165*, 106185, https://doi.org/10.1016/j.microc.2021.106185.
32. Kumar, Y.; Gupta, D.; Singh, P.P.; Kumar Das, D. Gadolinium ferrite nanoparticle based electrochemical sensor for detection of acetylsalicylic acid. *IOP Conference Series: Materials Science and Engineering* **2021**, *1116*, 012020, https://doi.org/10.1088/1757-899x/1116/1/012020.
33. Kumar, Y.; Pramanik, P.; Das, D.K. Electrochemical detection of paracetamol and dopamine molecules using nanoparticles of cobalt ferrite and manganese ferrite modified with graphite. *Heliyon* **2019**, *5*, e02031, https://doi.org/10.1016/j.heliyon.2019.e02031.
34. Mo, L.; Li, J.; Liu, Q.; Qiu, L.; Tan, W. Nucleic acid-functionalized transition metal nanosheets for biosensing applications. *Biosens Bioelectron* **2017**, *89*, 201-211, https://doi.org/10.1016/j.bios.2016.03.044.
35. Cui, L.; Fu, Y.; Liu, L.; Jiang, J.; Ding, Y.; Chen, L. Alkali metal–lanthanide co-encapsulated 19-tungsto-2-selenate derivative and its electrochemical detection of uric acid. *Inorganic Chemistry Communications* **2021**, *130*, 108734, https://doi.org/10.1016/j.inoche.2021.108734.
36. Chetankumar, K.; Swamy, B.E.K.; Naik, H.S.B. MgO and MWCNTs amplified electrochemical sensor for guanine, adenine and epinephrine. *Materials Chemistry and Physics* **2021**, *267*, 124610, https://doi.org/10.1016/j.matchemphys.2021.124610.
37. Manjula, N.; Chen, S.-M. One-pot synthesis of rod-shaped gadolinia doped zinc oxide decorated on graphene oxide composite as an efficient electrode material for isoprenaline sensor. *Composites Part B: Engineering* **2021**, *211*, 108631, https://doi.org/10.1016/j.compositesb.2021.108631.
38. Shabani-Nooshabadi, M.; Roostaee, M. Modification of carbon paste electrode with NiO/graphene oxide nanocomposite and ionic liquids for fabrication of high sensitive voltammetric sensor on sulfamethoxazole analysis. *Journal of Molecular Liquids* **2016**, *220*, 329-333, https://doi.org/10.1016/j.molliq.2016.05.001.
39. Raeisi-Kheirabadi, N.; Nezamzadeh-Ejhieh, A.; Aghaei, H. A brief study on the kinetic of the voltammetric behavior of the modified carbon paste electrode with NiO nanoparticles towards loratadine as a carboxylate-amidic drug compound. *Microchemical Journal* **2021**, *162*, 105869, https://doi.org/10.1016/j.microc.2020.105869.
40. Varma, A.; Mukasyan, A.S.; Rogachev, A.S.; Manukyan, K.V. Solution Combustion Synthesis of Nanoscale Materials. *Chemical Reviews* **2016**, *116*, 14493-14586, https://doi.org/10.1021/acs.chemrev.6b00279.

41. Kumar, Y.; Vashistha, V.K.; Sharma, V.; Patil, R.; Das, D.K. Manganese Ferrite Nanocomposite Modified Electrochemical Sensor for the Detection of Guanine and Uric Acid. *Analytical and Bioanalytical Electrochemistry* **2020**, *12*, 653-662.
42. Kumar, Y.; Pramanik, P.; Das, D.K. Electrochemical detection of paracetamol and dopamine molecules using nanoparticles of cobalt ferrite and manganese ferrite modified with graphite. *Heliyon* **2019**, *5*, e02031-e02031, https://doi.org/10.1016/j.heliyon.2019.e02031.
43.
43. Biswas, S.; Pradhan, S.; Naskar, H.; Bandyopadhyay, R.; Pramanik, P. Sol-gel synthesis of cubic titanium dioxide nanoparticle using poly(ethylene glycol) as a capping agent: voltammetric simultaneous determination of uric acid and guanine. *Microchimica Acta* **2018**, *185*, 513, https://doi.org/10.1007/s00604-018-3042-9.
44. Tadic, M.; Savic, S.M.; Jaglicic, Z.; Vojisavljevic, K.; Radojkovic, A.; Prsic, S.; Nikolic, D. Magnetic properties of $NiMn_2O_{4-\delta}$ (nickel manganite): Multiple magnetic phase transitions and exchange bias effect. *Journal of Alloys and Compounds* **2014**, *588*, 465-469, https://doi.org/10.1016/j.jallcom.2013.11.025.
45. Mazzara, F.; Patella, B.; Aiello, G.; O'Riordan, A.; Torino, C.; Vilasi, A.; Inguanta, R. Electrochemical detection of uric acid and ascorbic acid using r-GO/NPs based sensors. *Electrochimica Acta* **2021**, *388*, 138652, https://doi.org/10.1016/j.electacta.2021.138652.
46. Hui, Y.; Ma, X.; Hou, X.; Chen, F.; Yu, J. Silver nanoparticles-β-cyclodextrin-graphene nanocomposites based biosensor for guanine and adenine sensing. *Ionics* **2015**, *21*, 1751-1759, https://doi.org/10.1007/s11581-014-1343-5.
47. Yang, F.; Xie, Q.; Zhang, H.; Yu, S.; Zhang, X.; Shen, Y. Simultaneous determination of ascorbic acid, uric acid, tryptophan and adenine using carbon-supported $NiCoO_2$ nanoparticles. *Sensors and Actuators B: Chemical* **2015**, *210*, 232-240, https://doi.org/10.1016/j.snb.2014.12.120.
48. Wang, H.; Cao, T.; Wu, S.; Wang, S.; Yan, C.; Wang, Z.; Zhang, X.; Tong, Z. Synthesis of Novel Iron Porphyrin/Titanoniobate Nanocomposite for Electrochemical Detection of Uric Acid. *Journal of The Electrochemical Society* **2021**, *168*, 077509, https://doi.org/10.1149/1945-7111/ac139a.